Reversed interplay of quantum interference and which-way information in multiphoton entangled states

Young-Sik Ra,[1,*] Malte C. Tichy,[2] Hyang-Tag Lim,[1,†] Clemens Gneiting,[3,‡] Klaus Mølmer,[2] Andreas Buchleitner,[3] and Yoon-Ho Kim[1,§]

[1]*Department of Physics, Pohang University of Science and Technology (POSTECH), Pohang 790-784, Korea*

[2]*Department of Physics and Astronomy, University of Aarhus, 8000 Aarhus C, Denmark*

[3]*Physikalisches Institut, Albert-Ludwigs-Universität, Hermann-Herder-Straße 3, D-79104 Freiburg, Germany*

(Received 3 March 2017; published 22 August 2017)

We report experimental studies of quantum interference of multiphoton states impinging on a two-port balanced beam splitter. When the distinguishability between the two input paths is increased, we observe a reduction followed by a resurgence of the interference visibility in multiphoton coincidence detection. We ascribe this unusual behavior to the competition among contributions from distinct number state components of the interfering fields. Our results suggest that wave-particle duality gives rise to a wide range of largely unexplored phenomena in multiparticle interference.

DOI: 10.1103/PhysRevA.96.023845

I. INTRODUCTION

Quantum interference is one of the most fundamental features of quantum mechanics, observed in a variety of quantum systems [1–5]. A prototype example is the double-slit experiment where the repeated incidence of a single particle leaves wavelike interference fringes on a screen [1,6]. Perfect interference is observed only if no information is available about which path the particle has taken through the slits [7], whereas partial path distinguishability gradually reduces the fringe contrast [8–12] as a consequence of wave-particle duality [13,14]. The visibility of interference is, thus, often used to experimentally measure distinguishability associated with single-particle [8–12] or two-particle interference [2,15].

Recent technological development on generating and controlling multiple (more than two) photons has enabled observations of new features of quantum interference: e.g., multiphoton bunching [16,17], the genuine multiphoton phase [18,19], nonmonotonic quantum-to-classical transition [20], and detection-dependent coherence [21,22]. Interestingly, as interference of multiple photons cannot be simulated efficiently in classical ways, a quantum simulator based on multiphoton interference, boson sampling, has attracted a lot of attention as a step forward to simulate complex mathematical problems [23–26]. Furthermore, multiphoton interference is the key element for advanced optical sensing [27–30] and nonclassicality tests [31,32].

In contrast to single- or two-photon interference, we find that multiphoton interference exhibits a highly nontrivial behavior of the path distinguishability, even in the case of linear splitting and recombination of individual photons and, hence, of the corresponding annihilation and creation operators: Multiphoton interference fringes may vanish and reappear under gradually increased path distinguishability. We demonstrate this phenomenon with experiments on a two-mode three-photon entangled state. We show theoretically that the observed phenomena are not due to information erasure [33,34], non-Markovian processes [35,36], or a periodic decoherence [37,38] but due to a passage between different numbers of interfering photons [39]. For a separable multiphoton state, such different numbers of interfering photons result in different distributions of photons by interference [20], and for a multiphoton entangled state, they result in interference fringes with different phases, which gives rise to the observed reduction and resurgence of interference fringes. Multiphoton entangled states in general exhibit such a nontrivial relationship between interference fringes and which-path distinguishability with the exception of NOON states.

II. EXPERIMENTAL RESULTS

Figure 1(a) shows a schematic of our experimental setup to observe multiphoton interference. This setup, illuminated with the single-photon state,

$$|\psi_{1:0}\rangle = \frac{1}{\sqrt{2}}(|1,0\rangle_{a,b} + |0,1\rangle_{a,b}) \tag{1}$$

is equivalent to the aforementioned double-slit experiment [1,6], and single-photon detection at D_d, denoted as (0,1) detection, shows interference fringes as the interferometer phase θ is varied. When illuminated by a three-photon entangled state,

$$|\psi_{2:1}\rangle = \frac{1}{\sqrt{2}}(|2,1\rangle_{a,b} + |1,2\rangle_{a,b}), \tag{2}$$

we observe interference fringes in the coincidence detection of two photons at D_c and a single photon at D_d, denoted as (2,1) detection while scanning phase θ. In both the single- and the three-photon experiments, the distinguishability between paths a and b can be tuned by introducing a time-delay τ in path b: As τ increases, the path distinguishability becomes larger because the arrival time of a photon at the BS provides which-path information [10,13,14,20].

*Present address: Laboratoire Kastler Brossel, Université Pierre et Marie Curie, 75252 Paris, France. youngsikra@gmail.com

†Present address: Institute of Quantum Electronics, ETH Zurich, CH-8093 Zurich, Switzerland.

‡Present address: RIKEN, Wako-shi, Saitama 351-0198, Japan.

§yoonho72@gmail.com

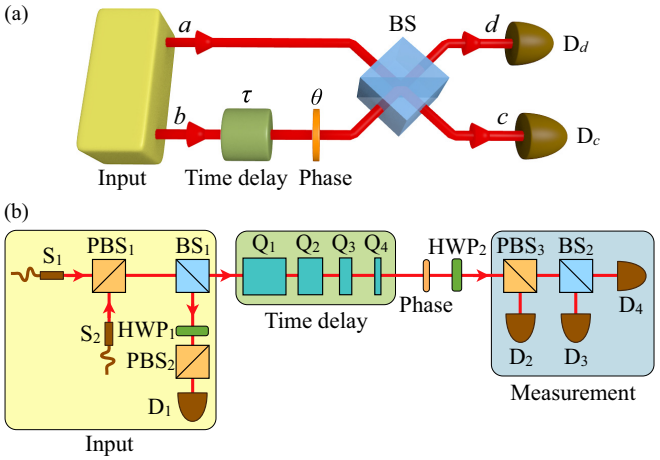

FIG. 1. (a) Schematic of an interferometer. BS is a nonpolarizing balanced beam splitter. D_c and D_d detect m and n photons, respectively, defining (m,n) detection. (b) Experimental setup. The path modes a and b are realized by horizontal and vertical polarization modes. Half-wave plates (HWP_1,HWP_2) are at 22.5°. Quartz plates Q_1, Q_2, Q_3, and Q_4 have different thicknesses of $7l$, $4l$, $2l$, and l (= 1.7 mm), respectively. The phase on the vertical polarization is controlled by rotating a HWP between two quarter-wave plates at 45° (not shown). D_1–D_4 are single-photon detectors. HWP_2 plays the role of the BS in (a).

In the experiment, we implement the interferometer by exploiting the horizontal and vertical polarization modes of a photon as sketched in Fig. 1(b). To prepare the single-photon state in Eq. (1) and the three-photon state in Eq. (2), we use photon pairs generated by spontaneous parametric down-conversion via type-I noncollinear phase matching [not shown in Fig. 1(b)]: a femtosecond pulse laser (duration: 150 fs; repetition rate: 95 MHz; central wavelength: 390 nm; average power: 190 mW) pumps a 2-mm-thick β-BaB_2O_4 crystal where each of the generated photons is filtered spectrally by a narrow bandpass filter (full width at half maximum of 3 nm) and spatially filtered by coupling into a single-mode fiber [S_1 or S_2 in Fig. 1(b)], which ensures indistinguishability among the generated photons. Photons from S_1 and S_2 are horizontally (H) and vertically (V) polarized, respectively, and arrive simultaneously at a polarizing beam splitter (PBS_1). The quantum state of the photons after PBS_1 is $(1-|\eta|^2)^{1/2}\sum_{n=0}^{\infty}\eta^n|n,n\rangle_{H,V}$ where we exploit the single-pair-term $|1,1\rangle_{H,V}$ and the two-pair-term $|2,2\rangle_{H,V}$ by detecting coincidence counts at D_1 and D_2 and D_1–D_4 (PerkinElmer SPCM-AQRH-13), respectively. To avoid contributions from higher-order photon-pair generation, we use low pump power (190 mW), which gives $|\eta|^2 = 0.02$. From the single-pair term (the two-pair term), the single-photon state in Eq. (1) [the three-photon state in Eq. (2)] is prepared by detecting a single photon at D_1 [41]. Time delays are implemented on the vertical polarization mode by using four different-thickness quartz plates (Q_1–Q_4), yielding time delays of 0, τ_0 (= 110 fs), ..., $7\tau_0$. For each time delay, we record single-photon interference fringes by detecting coincidence counts at D_1 and D_2 as well as three-photon interference fringes by detecting coincidence counts at D_1–D_4 while scanning the interferometer phase θ.

For single-photon interference, we observe a gradual reduction of the interference fringes in Figs. 2(a)–2(d) with increased time delays, summarized in Fig. 2(e). The straightforward and monotonic relation between the time delay and the visibility agrees well with the wave-particle duality relation [13,14]. In three-photon interference, however, we encounter in Figs. 2(f)–2(i) a qualitatively different behavior of the interference fringes, and, in particular, the three-photon interference vanishes at $\tau = 220$ fs [Fig. 2(h)] and reappears (with a π-phase shift) at a further increased time delay [Fig. 2(i)]. The behavior of the fringe visibility is summarized in Fig. 2(j).

III. THEORETICAL ANALYSIS

To explain why the three-photon interference exhibits the observed nontrivial behavior, we apply a multimode analysis for the multiphoton state. The creation operator for a photon occupying a Gaussian wave packet centered at time t can be described as

$$\mathcal{A}^\dagger = \frac{1}{\sqrt{\pi}\,\Delta\omega}\int d\omega\,\exp\left(-\frac{(\omega-\omega_0)^2}{2\,\Delta\omega^2}+i\omega t\right)\mathcal{A}_\omega^\dagger, \quad (3)$$

where $\mathcal{A}_\omega^\dagger$ is the creation operator of a photon with definite frequency ω, and ω_0 (= 2.41×10^{15} s^{-1}) and $\Delta\omega$ (= 3.99×10^{12} s^{-1}) are the central frequency and the bandwidth, respectively. The operator $\mathcal{A}^\dagger(\tau)$, creating a single photon in the wave packet with a time-delay τ, has a similar expression, and it can be expanded on the creation operator without delay $\mathcal{A}_0^\dagger$ and an orthogonal component, readily found by Gram-Schmidt orthonormalization [20,21,39],

$$\mathcal{A}^\dagger(\tau) = \alpha\mathcal{A}_0^\dagger + \beta\mathcal{A}_1^\dagger, \quad (4)$$

where $\mathcal{A}_1^\dagger$ is the creation operator of the orthonormalized mode, and

$$\alpha = e^{i\theta}\exp(-\Delta\omega^2\tau^2/4),$$
$$\beta = e^{i\theta}\sqrt{1-\exp(-\Delta\omega^2\tau^2/2)}, \quad (5)$$

with $\theta = \omega_0\tau$. $|\beta|^2(=1-|\alpha|^2)$ quantifies the path distinguishability [14,20], and it can be adjusted by the time delay τ: As τ increases, $|\beta|^2$ increases (consequently, $|\alpha|^2$ decreases), which results in a transition of $\mathcal{A}^\dagger(\tau)$ from $\mathcal{A}_0^\dagger$ to $\mathcal{A}_1^\dagger$. Note that other factors to increase the distinguishability (e.g., frequency, polarization, and spatial mode mismatches) can also induce the same transition [19].

Based on this decomposition, the single-photon state in Eq. (1) exposed to a time-delay τ in path b of the interferometer is described as

$$|\psi_{1:0}(\tau)\rangle = \left(\frac{1}{\sqrt{2}}|1,0\rangle_{a,b} + \frac{\alpha}{\sqrt{2}}|0,1\rangle_{a,b}\right) + \frac{\beta}{\sqrt{2}}|0,\widetilde{1}\rangle_{a,b}, \quad (6)$$

where a photon number without (with) a tilde denotes photons created by $\mathcal{A}_0^\dagger$ ($\mathcal{A}_1^\dagger$). The first two terms interfere at the BS, but the last term does not interfere with the first two as it describes a photon occupying an orthogonal mode. The time delay then induces a gradual transition from single-photon interference ($|\alpha|^2=1$, $|\beta|^2=0$) to no interference ($|\alpha|^2=0$, $|\beta|^2=1$).

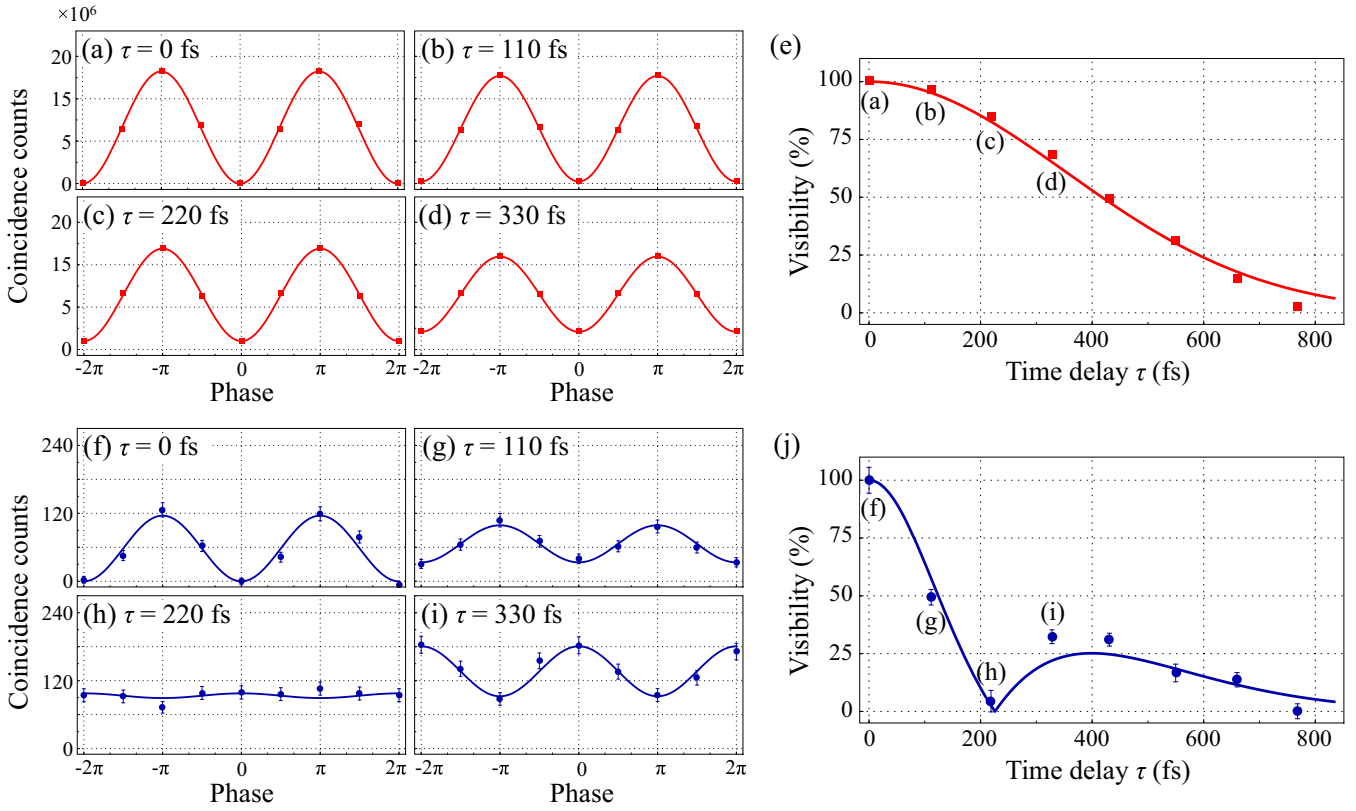

FIG. 2. Interference at various time delays. Single-photon interference fringes by $|1,0\rangle_{H,V} + |0,1\rangle_{H,V}$ are shown in (a)–(d), and the visibility is summarized in (e). Three-photon interference fringes by $|2,1\rangle_{H,V} + |1,2\rangle_{H,V}$ are shown in (f)–(i), and the visibility is summarized in (j). The red squares and blue dots are experimental data. For the single-photon interference, coincidence counts on D_1 and D_2 are recorded, and for the three-photon interference, coincidence counts on D_1–D_4 are recorded. Each of the data points in (a)–(d) and (f)–(i) is accumulated for 6600 s, and the noise counts estimated by an additional photon-pair generation are subtracted [40]. The error bars represent one standard deviation. The curves in (a)–(d) and (f)–(i) are sinusoidal fits of the experimental data. The red and blue curves in (e) and (j) are fits of the experimental data to the theoretical model in Eqs. (8) and (12).

The detection probability at D_d is given by

$$P_{(0,1)}(\tau) = \tfrac{1}{2}(1 - |\alpha| \cos\theta), \tag{7}$$

which yields a visibility of

$$V_{(0,1)}(\tau) = |\alpha|. \tag{8}$$

The detection probability is plotted in Fig. 3(a), which shows a gradual degradation of interference fringes as expected from the wave-particle duality relation [13,14].

The three-photon state in Eq. (2) is generated by the same creation operators and acquires a more complicated form when exposed to the time-delay τ,

$$|\psi_{2:1}(\tau)\rangle = \left(\frac{\alpha}{\sqrt{2}}|2,1\rangle_{a,b} + \frac{\alpha^2}{\sqrt{2}}|1,2\rangle_{a,b}\right) + \left(\frac{\beta}{\sqrt{2}}|2,\widetilde{1}\rangle_{a,b} + \alpha\beta|1,1\widetilde{1}\rangle_{a,b}\right) + \frac{\beta^2}{\sqrt{2}}|1,\widetilde{2}\rangle_{a,b}. \tag{9}$$

Here, qualitatively different interference types coexist: The first parentheses represent interference of three indistinguishable photons; the second represents interference of only two indistinguishable photons (the third photon occupying the orthogonal mode in path b); the last term does not lead to any interference. The three terms have different magnitudes as the time delay increases: Initially, $|2,1\rangle_{a,b}$ and $|1,2\rangle_{a,b}$ dominate, then $|1,1\widetilde{1}\rangle_{a,b}$ and $|2,\widetilde{1}\rangle_{a,b}$, and, finally $|1,\widetilde{2}\rangle_{a,b}$ dominates the

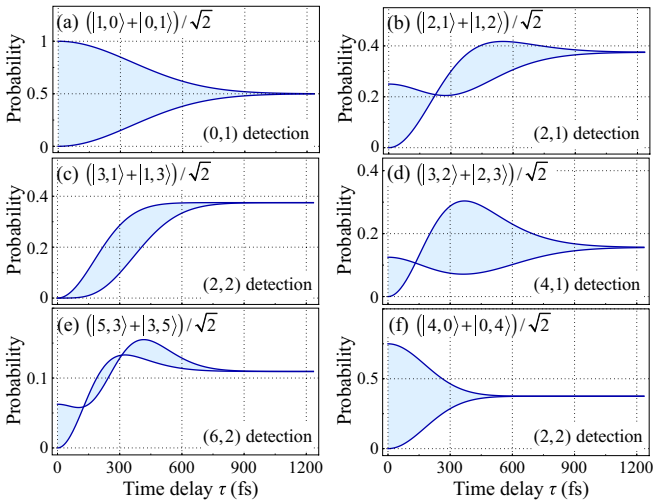

FIG. 3. Detection probabilities of input states versus a time delay. The shaded areas represent interference fringes with a period of ω_0 for (a), (b), and (d), $2\omega_0$ for (c) and (e), and $4\omega_0$ for (f).

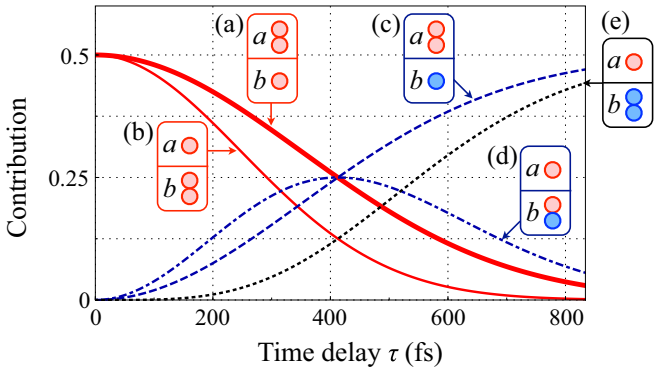

FIG. 4. Contribution of each term in Eq. (9). (a) $|2,1\rangle_{a,b}$ and (b) $|1,2\rangle_{a,b}$ can interfere at the BS in Fig. 1(a). Similarly, (c) $|2,\widetilde{1}\rangle_{a,b}$ and (d) $|1,\widetilde{1}\widetilde{1}\rangle_{a,b}$ can interfere. (e) $|1,\widetilde{2}\rangle_{a,b}$ is not involved in any interference. The red and blue disks represent photons created by $\mathcal{A}_0^\dagger$ and $\mathcal{A}_1^\dagger$, respectively.

state, see Fig. 4. As a result, the time delay displays a transition from three-photon interference over two-photon interference to no interference. The (2,1) detection probability, plotted in Fig. 3(b), is thus given by

$$P_{(2,1)}(\tau) = P^{(\mathrm{three})}(\tau) + P^{(\mathrm{two})}(\tau) + P^{(\mathrm{no})}(\tau), \tag{10}$$

where

$$\begin{aligned} P^{(\mathrm{three})}(\tau) &= |\alpha|^2(|\alpha|^2 - 2|\alpha|\cos\theta + 1)/16, \\ P^{(\mathrm{two})}(\tau) &= |\beta|^2(4|\alpha|^2 + 4|\alpha|\cos\theta + 3)/16, \\ P^{(\mathrm{no})}(\tau) &= 3|\beta|^4/16, \end{aligned} \tag{11}$$

and the visibility becomes

$$V_{(2,1)}(\tau) = \frac{|\alpha(2-3|\alpha|^2)|}{3-2|\alpha|^2}. \tag{12}$$

We can now see that the vanishing and reappearance of interference fringes shown in Fig. 3(b) are due to the π phase difference [see Figs. 2(f)–2(i)] between the three-photon and the two-photon interference fringes $P^{(\mathrm{three})}(\tau)$ and $P^{(\mathrm{two})}(\tau)$. First the three-photon interference dominates, but for a critical delay, the three- and two-photon interference signals add to a constant, whereas for larger delay the two-photon interference dominates until, eventually, the detection probability is governed by the no-interference-type $P^{(\mathrm{no})}(\tau)$.

IV. DISCUSSION

As we have seen, multiphoton interference exhibits a nontrivial dependence on the path distinguishability because of the different numbers of interfering photons contributing to the overall interference signal. Using our creation operators and their expansion on orthonormal modes, we can account for the time-delay τ at mode b for any linear combination of input Fock states on the interferometer. Let us, for example, consider the $(N+M)$-photon state $|\psi_{N:M}\rangle = (|N,M\rangle_{a,b} + |M,N\rangle_{a,b})/\sqrt{2}$, where $N > M$. After the action of the time delay, this state can be written as

$$\begin{aligned} |\psi_{N:M}(\tau)\rangle = \frac{1}{\sqrt{2}}\sum_{k=0}^{M}\sqrt{\binom{M}{k}}\alpha^{M-k}\beta^k|N,(M-k)\tilde{k}\rangle_{a,b} \\ + \frac{1}{\sqrt{2}}\sum_{l=0}^{N}\sqrt{\binom{N}{l}}\alpha^{N-l}\beta^l|M,(N-l)\tilde{l}\rangle_{a,b}, \end{aligned} \tag{13}$$

which leads to interference contributions from states with total photon numbers in the "nontilded" modes created by $\mathcal{A}_0^\dagger$, ranging from N to $N+M$. Figures 3(c)–3(f) show different examples of interference fringes as a function of the time delay. For a four-photon state $(|3,1\rangle_{a,b} + |1,3\rangle_{a,b})/\sqrt{2}$, interference fringes by (2,2) detection is shown in Fig. 3(c). At zero time delay, no interference fringe appears because neither $|3,1\rangle_{a,b}$ nor $|1,3\rangle_{a,b}$ can be detected by (2,2) detection [21,42]; however, when the time delay is introduced, interference fringes from three indistinguishable photons emerge. Another example shown in Fig. 3(d) is a five-photon state $(|3,2\rangle_{a,b} + |2,3\rangle_{a,b})/\sqrt{2}$ measured by (4,1) detection. Similar to the three-photon state in Eq. (2), the five-photon state exhibits vanishing and reappearance of interference. An eight-photon state $(|5,3\rangle_{a,b} + |3,5\rangle_{a,b})/\sqrt{2}$ exhibits a more complex behavior when measured by (6,2) detection: Vanishing and reappearance of interference take place twice, shown in Fig. 3(e). Remarkably, states $|\psi_{N:M}\rangle$ with $M > 0$ in Figs. 3(c)–3(e) show a higher tolerance to the path distinguishability than the NOON state $|\psi_{N:0}\rangle$ in Fig. 3(f), which always shows a simple and rapid reduction of the fringe visibility, even though the former contains a larger or equal number of photons than the latter.

V. CONCLUSION

The observed vanishing and reappearance of multiphoton interference in the path distinguishability transition is due to contributions to the overall interference signal from different numbers of interfering photons, and the observation clearly demonstrates that multiphoton interference exhibits a qualitatively different behavior from single-photon interference, which is governed by the wave-particle duality [13,14]. Our results, on one hand, provide a different characteristic of multiphoton interference [39,43], and, on the other hand, they may inspire investigation of a more foundational character, cf. the different view on wave-particle duality in first and second quantizations [13,14,44,45].

From a practical perspective, quantum technologies, such as precision measurements [27–30] and quantum simulations [24–26] increasingly are based on multiphoton interference and entanglement. It is, hence, pertinent to understand how these phenomena are affected by the nontrivial dependence on distinguishability.

ACKNOWLEDGMENTS

This work was supported by the National Research Foundation of Korea (Grants No. 2016R1A2A1A05005202 and No. 2016R1A4A1008978), by the Danish Council for

Independent Research, and by the Villum Foundation. C.G. and A.B. gratefully acknowledge support by DAAD (within the PAJAKO program) through funds of the German Federal Foreign Office.

[1] P. Grangier, G. Roger, and A. Aspect, Europhys. Lett. **1**, 173 (1986).
[2] C. K. Hong, Z. Y. Ou, and L. Mandel, Phys. Rev. Lett. **59**, 2044 (1987).
[3] S. Gerlich, S. Eibenberger, M. Tomandl, S. Nimmrichter, K. Hornberger, P. J. Fagan, J. Tüxen, M. Mayor, and M. Arndt, Nat. Commun. **2**, 263 (2011).
[4] E. Bocquillon, V. Freulon, J. M. Berroir, P. Degiovanni, B. Placais, A. Cavanna, Y. Jin, and G. Feve, Science **339**, 1054 (2013).
[5] R. Lopes, A. Imanaliev, A. Aspect, M. Cheneau, D. Boiron, and C. I. Westbrook, Nature (London) **520**, 66 (2015).
[6] R. Feynman, R. B. Leighton, and M. L. Sands, *The Feynman Lectures on Physics* (Addison-Wesley, Reading, MA, 1965), Vol. III.
[7] T. B. Pittman, D. V. Strekalov, A. Migdall, M. H. Rubin, A. V. Sergienko, and Y. H. Shih, Phys. Rev. Lett. **77**, 1917 (1996).
[8] J. G. Rarity, P. R. Tapster, E. Jakeman, T. Larchuk, R. A. Campos, M. C. Teich, and B. E. A. Saleh, Phys. Rev. Lett. **65**, 1348 (1990).
[9] S. Dürr, T. Nonn, and G. Rempe, Phys. Rev. Lett. **81**, 5705 (1998).
[10] P. D. D. Schwindt, P. G. Kwiat, and B.-G. Englert, Phys. Rev. A **60**, 4285 (1999).
[11] L. Hackermüller, K. Hornberger, B. Brezger, A. Zeilinger, and M. Arndt, Nature (London) **427**, 711 (2004).
[12] V. Jacques, E. Wu, F. Grosshans, F. Treussart, P. Grangier, A. Aspect, and J. F. Roch, Phys. Rev. Lett. **100**, 220402 (2008).
[13] G. Jaeger, A. Shimony, and L. Vaidman, Phys. Rev. A **51**, 54 (1995).
[14] B. G. Englert, Phys. Rev. Lett. **77**, 2154 (1996).
[15] P. J. Mosley, J. S. Lundeen, B. J. Smith, P. Wasylczyk, A. B. U'Ren, C. Silberhorn, and I. A. Walmsley, Phys. Rev. Lett. **100**, 133601 (2008).
[16] Z. Y. Ou, J.-K. Rhee, and L. J. Wang, Phys. Rev. Lett. **83**, 959 (1999).
[17] N. Spagnolo, C. Vitelli, L. Aparo, P. Mataloni, F. Sciarrino, A. Crespi, R. Ramponi, and R. Osellame, Nat. Commun. **4**, 1606 (2013).
[18] S. Agne, T. Kauten, J. Jin, E. Meyer-Scott, J. Z. Salvail, D. R. Hamel, K. J. Resch, G. Weihs, and T. Jennewein, Phys. Rev. Lett. **118**, 153602 (2017).
[19] A. J. Menssen, A. E. Jones, B. J. Metcalf, M. C. Tichy, S. Barz, W. S. Kolthammer, and I. A. Walmsley, Phys. Rev. Lett. **118**, 153603 (2017).
[20] Y.-S. Ra, M. C. Tichy, H.-T. Lim, O. Kwon, F. Mintert, A. Buchleitner, and Y.-H. Kim, Proc. Natl. Acad. Sci. USA **110**, 1227 (2013).
[21] Y.-S. Ra, M. C. Tichy, H.-T. Lim, O. Kwon, F. Mintert, A. Buchleitner, and Y.-H. Kim, Nat. Commun. **4**, 2451 (2013).
[22] R.-B. Jin, M. Fujiwara, R. Shimizu, R. J. Collins, G. S. Buller, T. Yamashita, S. Miki, H. Terai, M. Takeoka, and M. Sasaki, Sci. Rep. **6**, 36914 (2016).
[23] S. Aaronson and A. Arkhipov, *Proceedings of the 43rd ACM Symposium on Theory of Computing* (ACM, New York, 2011), pp. 333–342.
[24] M. C. Tichy, J. Phys. B: At. Mol. Opt. Phys. **47**, 103001 (2014).
[25] M. Tillmann, S.-H. Tan, S. E. Stoeckl, B. C. Sanders, H. de Guise, R. Heilmann, S. Nolte, A. Szameit, and P. Walther, Phys. Rev. X **5**, 041015 (2015).
[26] J. Carolan, C. Harrold, C. Sparrow, E. Martín-López, N. J. Russell, J. W. Silverstone, P. J. Shadbolt, N. Matsuda, M. Oguma, M. Itoh, G. D. Marshall, M. G. Thompson, J. C. F. Matthews, T. Hashimoto, J. L. O'brien, and A. Laing, Science **349**, 711 (2015).
[27] V. Giovannetti, S. Lloyd, and L. Maccone, Nat. Photonics **5**, 222 (2011).
[28] P. C. Humphreys, M. Barbieri, A. Datta, and I. A. Walmsley, Phys. Rev. Lett. **111**, 070403 (2013).
[29] M. C. Tichy, Y.-S. Ra, H.-T. Lim, C. Gneiting, Y.-H. Kim, and K. Mølmer, New J. Phys. **17**, 023008 (2015).
[30] Y.-S. Ra, H.-T. Lim, J.-E. Oh, and Y.-H. Kim, Opt. Express **23**, 30807 (2015).
[31] E. V. Shchukin and W. Vogel, Phys. Rev. A **72**, 043808 (2005).
[32] C. Erven, E. Meyer-Scott, K. Fisher, J. Lavoie, B. L. Higgins, Z. Yan, C. J. Pugh, J. P. Bourgoin, R. Prevedel, L. K. Shalm, L. Richards, N. Gigov, R. Laflamme, G. Weihs, T. Jennewein, and K. J. Resch, Nat. Photonics **8**, 292 (2014).
[33] P. G. Kwiat, A. M. Steinberg, and R. Y. Chiao, Phys. Rev. A **45**, 7729 (1992).
[34] Y.-H. Kim, R. Yu, S. P. Kulik, Y. Shih, and M. O. Scully, Phys. Rev. Lett. **84**, 1 (2000).
[35] J.-S. Xu, C.-F. Li, M. Gong, X.-B. Zou, C.-H. Shi, G. Chen, and G.-C. Guo, Phys. Rev. Lett. **104**, 100502 (2010).
[36] R. Lo Franco, B. Bellomo, S. Maniscalco, and G. Compagno, Int. J. Mod. Phys. B **27**, 1345053 (2013).
[37] R. Lo Franco, B. Bellomo, E. Andersson, and G. Compagno, Phys. Rev. A **85**, 032318 (2012).
[38] J.-S. Xu, K. Sun, C.-F. Li, X.-Y. Xu, G.-C. Guo, E. Andersson, R. Lo Franco, and G. Compagno, Nat. Commun. **4**, 2851 (2013).
[39] M. C. Tichy, H.-T. Lim, Y.-S. Ra, F. Mintert, Y.-H. Kim, and A. Buchleitner, Phys. Rev. A **83**, 062111 (2011).
[40] B. H. Liu, F. W. Sun, Y. X. Gong, Y. F. Huang, Z. Y. Ou, and G. C. Guo, Phys. Rev. A **77**, 023815 (2008).
[41] Y.-S. Ra, H.-T. Lim, and Y.-H. Kim, Phys. Rev. A **94**, 042329 (2016).
[42] R. A. Campos, B. E. A. Saleh, and M. C. Teich, Phys. Rev. A **40**, 1371 (1989).
[43] J.-W. Pan, Z.-B. Chen, C.-Y. Lu, H. Weinfurter, A. Zeilinger, and M. Zukowski, Rev. Mod. Phys. **84**, 777 (2012).
[44] J.-H. Huang, S. Wölk, S.-Y. Zhu, and M. S. Zubairy, Phys. Rev. A **87**, 022107 (2013).
[45] K. Banaszek, P. Horodecki, M. Karpiński, and C. Radzewicz, Nat. Commun. **4**, 2594 (2013).